Electronic Supplementary Information

Combining API in a dual-drug ternary cocrystal approach

Lixing Song,[a] Koen Robeyns,[a] Nikolay Tumanov,[b] Johan Wouters,[b] and Tom Leyssens[a]

[a]*Institute of Condensed Matter and Nanosciences, Université catholique de Louvain, 1 Place Louis Pasteur, B-1348 Louvain-La-Neuve, Belgium, E-mail: tom.leyssens@uclouvain.be*

[b]*Unité de Chimie Physique Théorique et Structurale, Chemistry Department, Namur Institute of Structured Matter (NISM), University of Namur, 61 rue de Bruxelles, B-5000 Namur, Belgium.*

Contents

Abbreviation of cocrystal forms

ICC1	$LEV_2{\cdot}CaCl_2{\cdot}2H_2O$
ICC2	$INA_2{\cdot}CaCl_2{\cdot}4H_2O$
ICC3	$NA_2{\cdot}CaCl_2{\cdot}2H_2O$
ICC4	$ETI_2{\cdot}CaCl_2{\cdot}2H_2O$
TICC1	$ETI_2{\cdot}INA{\cdot}CaCl_2{\cdot}H_2O$
TICC2	$LEV_2{\cdot}INA{\cdot}CaCl_2{\cdot}H_2O$
TICC3	$LEV_2{\cdot}NA{\cdot}CaCl_2{\cdot}H_2O$

Materials and methods

Starting Materials. LEV was purchased from Xiamen Top Health Biochem Tech. Co. Ltd. ETI was prepared by racemization of LEV. 10 g of LEV together with catalytic amount (0.05 eq.) of MeONa were added to 10 mL of methanol. The solution was refluxed under continuous stirring for 24 h, and then cooled to room temperature. The compound crystallizes spontaneously. After filtration, the product was washed twice with methanol. The recovered product was used as such (XRPD is consistent with the calculated one and no impure signals). Calcium chloride anhydrous powder (96% pure), NA (99% pure) and INA (99% pure) was purchased from ACROS. pH 1.2 HCl aqueous solution was prepared by diluting 8.3 mL concentrated HCl into 1000 mL aqueous solution. All the solvents were reagent grade. They are all used without further purification.

Liquid Assisting Grinding (LAG). Powder samples can be obtained mechanochemically through LAG of different stoichiometric mixtures of LEV or ETI (+/- 30mg), INA or NA, and $CaCl_2$, with the addition of 4 stainless-steel balls and 20 μL methanol. The sample was ground in a RETSCH Mixer Mill MM 400 for 90 min with a beating frequency of 30 Hz.

Solution experiments. All the single crystals were prepared by dissolution of the starting materials ETI/LEV, NA/INA and $CaCl_2$ in 2:1:1 (TICC2 and TICC3) or 2:2:1 (TICC1, also could be re-prepared under 2:1:1) stoichiometry in methanol. The solutions were then left to evaporate at room temperature seeding with the powders obtained from the LAG experiments.

Slurry experiments. The slurry experiments for the cocrystal screening were performed by stirring the suspensions of the starting materials in methanol. The stoichiometric ratios of

ETI/LEV:INA/NA:$CaCl_2$ were selected as 1:1:1, 2:2:1, 2:1:1, 1:2:1, 4:1:1, 4:2:1, 1:4:1 and 2:4:1. The total mass of starting materials was 100 mg. The amount of methanol was set at 80 μL. The suspensions were seeded with starting materials and corresponding cocrystals (from LAG experiments) and stirred at 25 °C for over 48 h to make sure the system reached thermodynamic equilibrium. Then samples were filtered over sintered glass, followed by XRPD analysis of the solid phases. The results are shown in Table S1.

The slurry experiments for congruency testing were performed by stirring suspensions of starting materials in different solvents under the stoichiometry of the specific cocrystal LEV-$CaCl_2$ (2:1), ETI-$CaCl_2$ (2:1),INA-$CaCl_2$ (2:1), NA-$CaCl_2$ (2:1), ETI-INA-$CaCl_2$ (2:1:1), LEV-INA-$CaCl_2$ (2:1:1) and LEV-NA-$CaCl_2$ (2:1:1). The total mass of starting material was 100 mg. The solvents were selected as H_2O, methanol, ethanol, acetone, isopropanol, chloroform, dichloromethane, acetonitrile, ethyl acetate, toluene, hexane and pH 1.2 HCl aqueous solution. We made sure the amount of solvent added did not lead to full dissolution. The suspensions were seeded with starting materials and corresponding cocrystals and stirred at 25 °C for over 48 h to make sure the system reached thermodynamic equilibrium. Then samples were filtered over sintered glass, followed by XRPD analysis of the solid phases. The results are shown in Table S4.

Solubility measurement. If the cocrystal system was found congruent for a given solvent, the particular cocrystal is the only stable solid phase in suspension at equilibrium. Thus, in solution the compounds show the same stoichiometry as the cocrystal solid phase Solubility measurement were performed by gravimetric method. A suspension of starting materials under corresponding stoichiometry was created and left to stir for 48 h at 25 °C. Supernatant was removed, weighed and left at 105 °C for a few days until the weight did not decrease any longer (complete solvent removal). This is confirmed by TGA analysis, showing a weight loss of less than 1% up to 160 °C, showing full solvent removal. By mass balance and knowing the stoichiometry of the solid, the solubility of each parent compound is obtained. The experiments were repeated three times and the average taken.

X-Ray Powder diffraction (XRPD) and Variable Temperature X-Ray Powder diffraction (VT-XRPD). X-ray powder diffraction data were collected with a Siemens D5000 diffractometer equipped with a Cu X-ray source operating at 40 kV and 40 mA and the secondary monochromator allowing to select the Kα radiation of Cu (λ = 1.5418 Å). A scanning range of 2θ values from 5° to 50° at a scan rate of 0.6° min^{-1} was applied. VT-XRPD was performed using an X'pert PRO PANalytical diffractometer (2θ scanned from 4 to 40°, CuKα radiation, Bragg–Brentano geometry) and an Anton Paar TTK 450 system for measurement at controlled temperature. Thermal programs were selected based on TGA results.

Single crystal X-ray diffraction (SC-XRD). Data collection was carried out on a MAR345 using monochromated MoKα radiation (λ = 0.71073 Å) (Xenocs Fox3D mirror) produced by a Rigaku UltraX18S rotating anode at room temperature.

Differential scanning calorimetry (DSC). DSC measurements were performed on a TA DSC2500 with Tzero technology calibrated with indium under 50 mL/min continuous nitrogen flow. Samples were prepared in aluminium Tzero pans with punctured hermetic lid. The temperature profile applied starts at 30 °C and increases up to 160 °C with a rate of 2 °C /min.

Thermogravimetric analysis (TGA). TGA measurements were performed on a Mettler Toledo TGA /SDTA851^e using an alumina crucible. The heating profile applied starts at 25 ° C and goes up to 300 °C with a rate of 2 °C /min under continuous nitrogen flow of 50.0 mL/min.

Cocrystal screening

The stoichiometry of LAG experiments was first selected as 2:2:1 (ETI/LEV:INA/NA:$CaCl_2$) based on the stoichiometry of binary ICCs. After confirming the appearance of new forms by XRPD, the single crystals were prepared under the stoichiometric ratio of 2:2:1 in methanol with seeding, resulting in single crystals with the stoichiometry of 2:1:1. Thus, we measured the LAG experiments under a 2:1:1 ratio as well conforming the excess INA/NA in the initial 2:2:1 samples. As no TICC formation was observed for the ETI-NA-$CaCl_2$ system, grinding experiments were furthermore performed under the ratios 4:2:1, 4:1:1, 2:4:1, 2:2:1, 2:1:1, 1:1:1, 1:2:1, 1:4:1. All however led to a mixture of ICC4 and NA. It should be mentioned that a polymorphic transformation of ETI occurs in some cases during the LAG process as temperatures fluctuate around the transition temperature for this enantiotropically related system.[1] The results are shown in XRPD overlays.

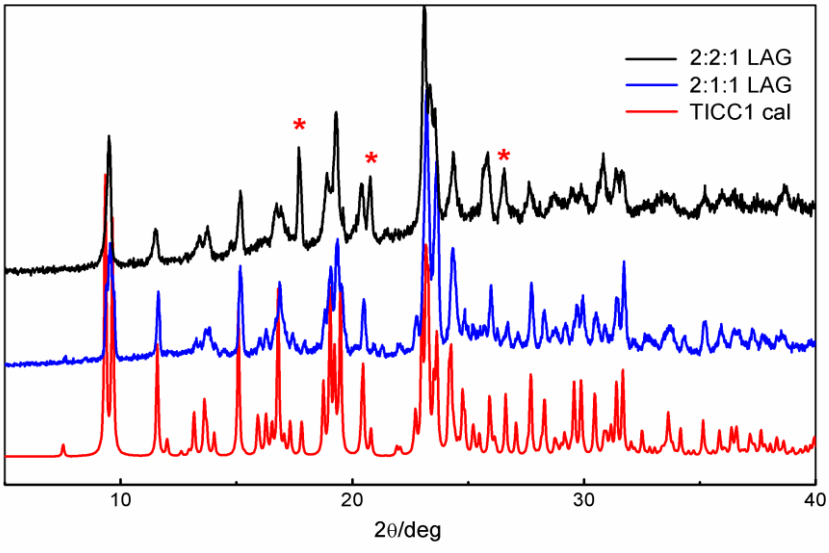

Figure S1. LAG results for the ETI-INA-$CaCl_2$ system. LAG of 2:2:1 ratio (black); LAG of 2:1:1 ratio (blue); simulated XRPD from single crystal (red). Some corresponding peaks of INA are marked with asterisks.

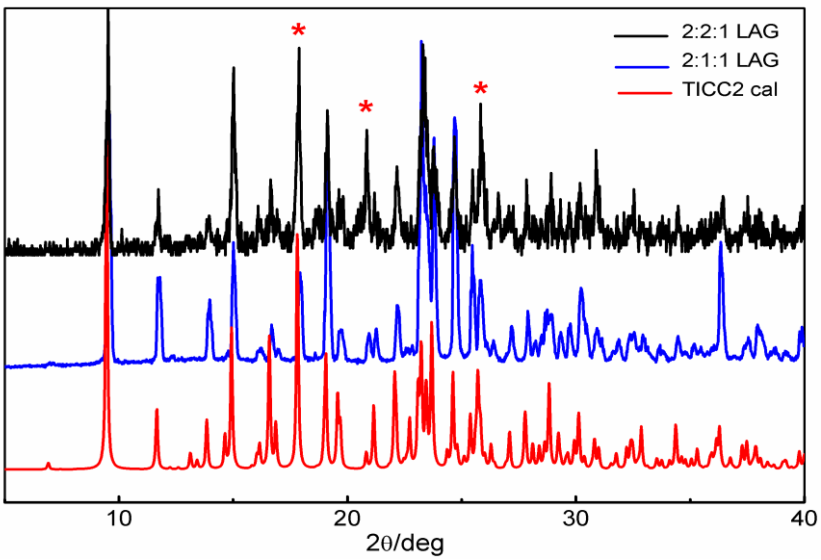

Figure S2. LAG results for the LEV-INA-$CaCl_2$ system. LAG of 2:2:1 ratio (black); LAG of 2:1:1 ratio (blue); simulated XRPD from single crystal (red). Some corresponding peaks of INA are marked with asterisks.

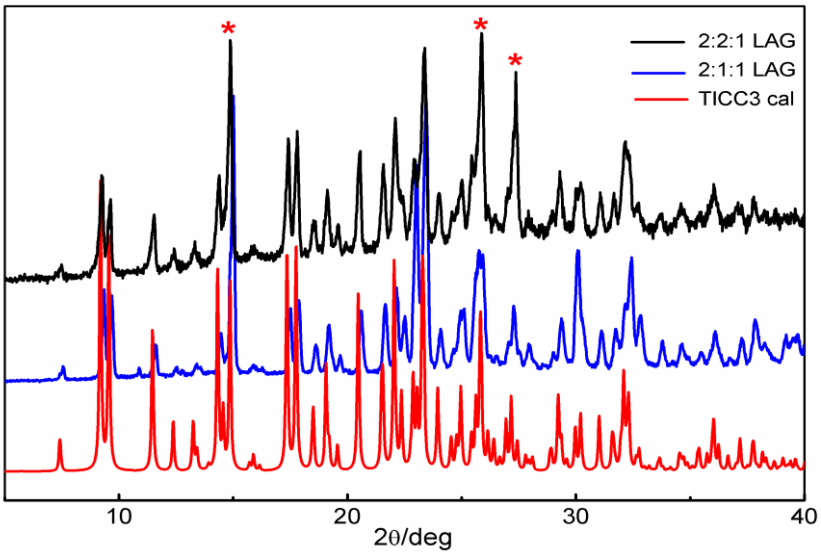

Figure S3. LAG results for the LEV-NA-$CaCl_2$ system. LAG of 2:2:1 ratio (black); LAG of 2:1:1 ratio (blue); simulated XRPD from single crystal (red). Some corresponding peaks of NA are marked with asterisks.

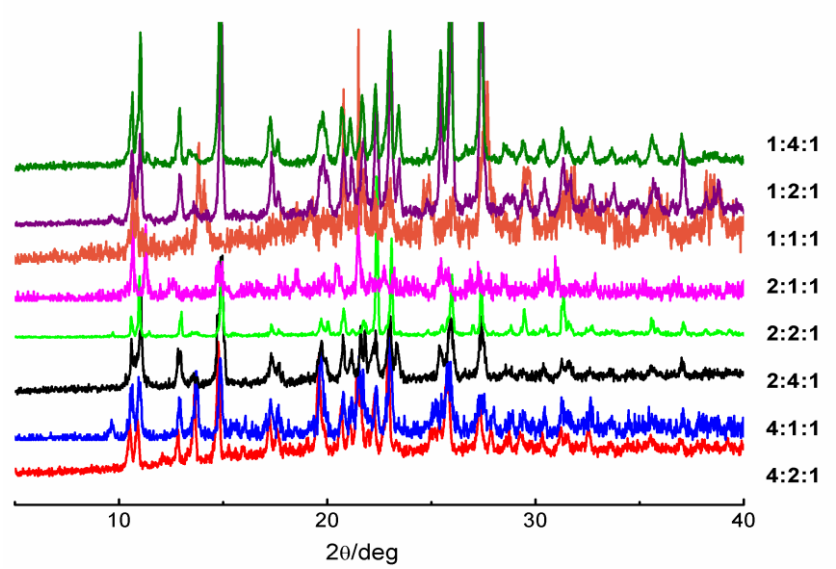

Figure S4. LAG results for the ETI-NA-$CaCl_2$ system.

To check all the possible cocrystal forms and to determine the most stable form, slurry experiments under different stoichiometries in methanol were conducted. There was not any new crystal form coming out. The slurry results are shown in Table S.1.

Table S1. The results of slurry screening experiments for ternary systems.

ratio	ETI+INA+ $CaCl_2$	LEV+INA+$CaCl_2$	LEV+NA+$CaCl_2$	ETI+NA+ $CaCl_2$
1:1:1	TICC1+ICC4	TICC2	TICC3+ICC1	ICC3+ICC4
2:2:1	TICC1	TICC2	TICC3	ICC4+NA
2:1:1	TICC1	TICC2	TICC3+ICC1	ICC4
1:2:1	TICC1	TICC2	TICC3+ICC3	ICC3+ICC4
4:1:1	TICC1+ETI	TICC2+LEV	LEV	ICC4+ETI
4:2:1	TICC1+ETI	TICC2+LEV	ICC1+ICC3	ETI
1:4:1	INA	INA	NA	ICC3+NA
2:4:1	TICC1+INA	TICC2+INA	TICC3+NA	NA

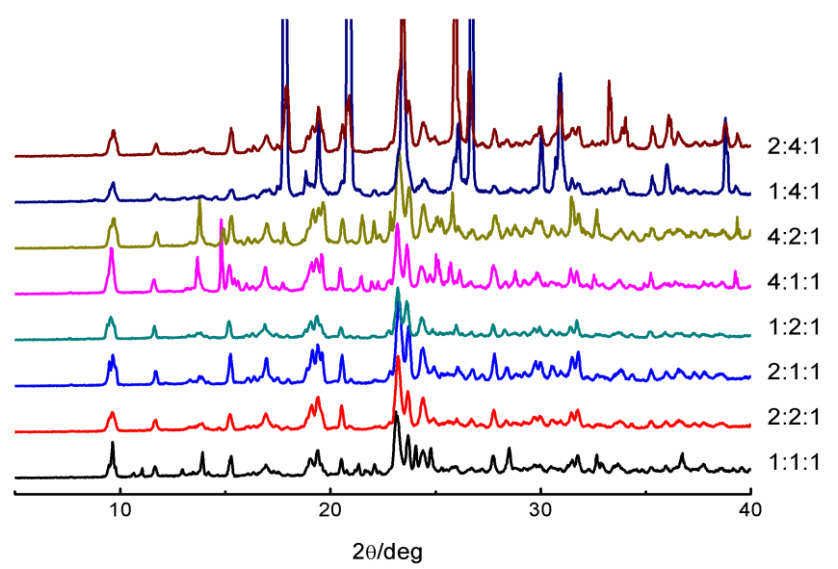

Figure S5. Slurry results for the ETI-INA-$CaCl_2$ system.

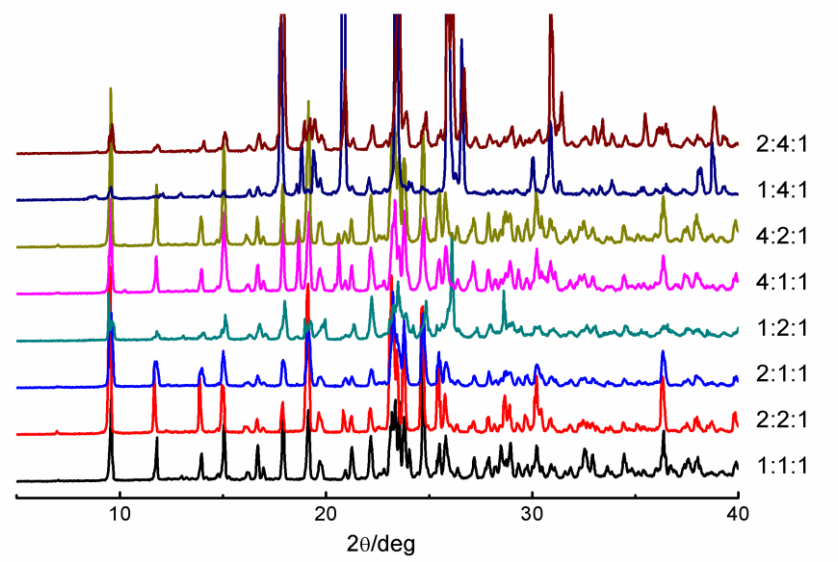

Figure S6. Slurry results for the LEV-INA-$CaCl_2$ system.

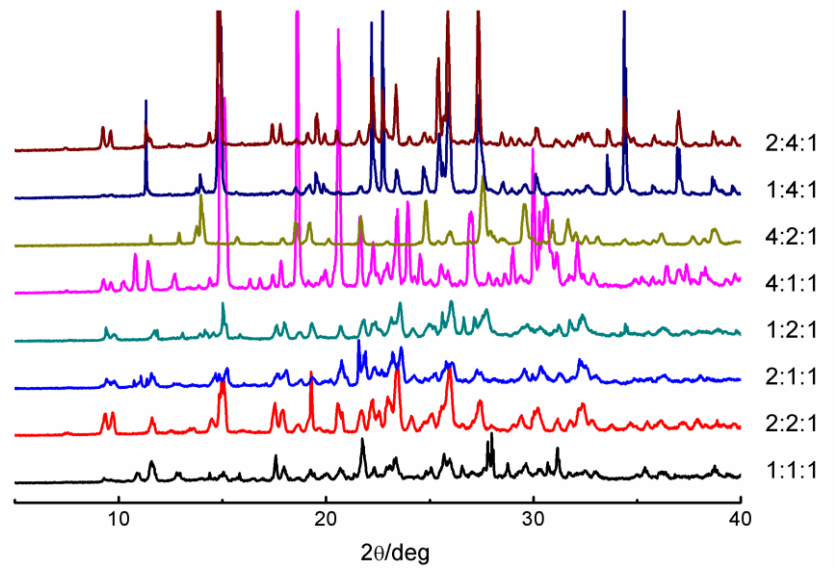

Figure S7. Slurry results for the LEV-NA-$CaCl_2$ system.

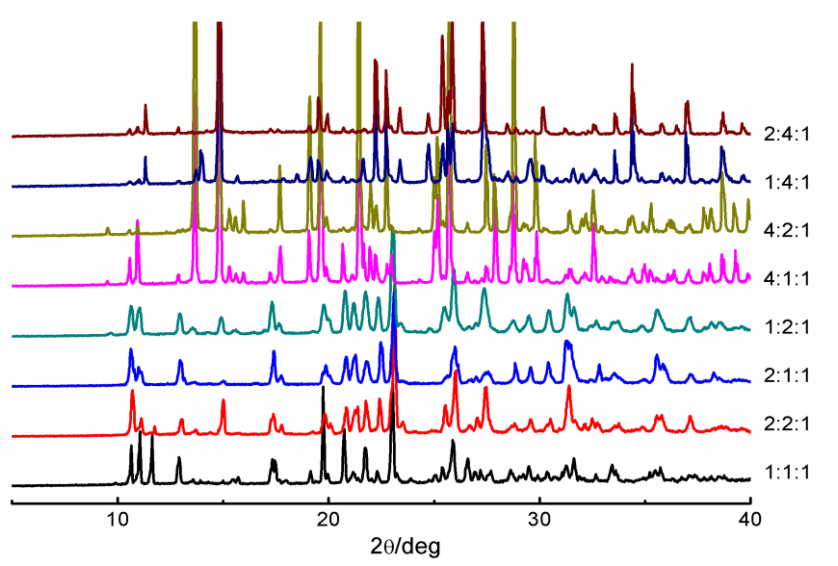

Figure S8. Slurry results for the ETI-NA-$CaCl_2$ system.

Structural characteristics

Table S2. Crystal data and refinement parameters for the three TICCs.

	TICC1	TICC2	TICC3
Chemical formula	$C_{22}H_{36}Cl_2N_6O_6Ca$	$C_{22}H_{36}Cl_2N_6O_6Ca$	$C_{22}H_{36}Cl_2N_6O_6Ca$
M_r, g*mol^{-1}	591.55	591.55	591.55
T / K	293(2)	293(2)	296(2)
Wavelength Å	MoKα	MoKα	MoKα
Crystal system	Triclinic	Orthorhombic	Monoclinic

Space group	*P-1*	*P 2_1 2_1 2_1*	*P 2_1*
a /Å	7.968(2)	7.9303(11)	11.9243(5)
b /Å	12.170 (4)	15.1768(2)	8.0669(3)
c /Å	15.304(4)	23.7226(3)	15.4348(7)
α / °	87.17(2)	90	90
β / °	86.30 (2)	90	92.338(4)
γ / °	74.76(2)	90	90
V /Å^3	1428.0(7)	2855.17(7)	1483.46(11)
Z	2	4	2
ρ / mg.cm^{-3}	1.376	1.376	1.324
μ / mm^{-1}	0.453	0.453	0.436
Measd reflns	3208	19720	11004
Indep reflns	3208	5423	5624
Reflns with $I > 2\sigma(I)$	2033	5133	4624
R indices [I>2σ(I)]	R_1 = 0.0989, wR_2 = 0.2139	R_1 = 0.0293, wR_2 = 0.0709	R_1 = 0.0433, wR_2 = 0.0900
R indices (all data)	R_1 = 0.1544, wR_2 = 0.2391	R_1 = 0.0317, wR_2 = 0.0725	R_1 = 0.0581, wR_2 = 0.0959
Absolute structure parameter	-	-0.028(19)	0.02(3)

Data collection was performed on a Mar345 image plate using MoKa radiating generated by a Rigaku Ultra X 18S rotating anode equipped with Fox3D mirrors. Data integration and reduction was performed by CrysAlisPRO[2]. Structures were solved by SHELXT[3] and refined by full-matrix least-squares on F^2 using SHELXL2014/7[4]. All non-hydrogen atoms were refined anisotropically and hydrogen atoms were placed at calculated positions in riding mode, with temperature factors set at 1.2 times U_{eq} of the parent atoms, 1.5 for methyl and OH hydrogens. TICC1 was diffracted poorly and a resolution cut-off was imposed during structure refinement. Furthermore, TICC1 was found to be twinned and refinement was continued against HKLF5 formatted data (PLATON twinrotmat[5]). The ethyl moieties in TICC1 were found to be disordered as well as an amide group in TICC3, and were refined in two distinct parts.

CCDC 2025075-2025077 contain the supplementary crystallographic data for this paper. These data can be obtained free of charge from The Cambridge Crystallographic Data Centre via www.ccdc.cam.ac.uk/structures

Table S3. Hydrogen bond lengths/Å and angles/° for all TICCs.

D-H···A	d (D-H)	d (H···A)	d (D···A)	∠DHA
TICC1				

O4-H4A···Cl2 [i]	0.82	2.42	3.048	134
O4-H4B···Cl3 [ii]	0.82	2.26	3.062	165
N20-H20B···Cl2 [i]	0.86	2.47	3.250	151
N40-H40A···Cl2 [i]	0.86	2.57	3.352	151
N40-H40B···Cl3 [i]	086	2.51	3.259	145
N53-H53B···Cl3 [iii]	0.86	2.62	3.420	155
Symmetry codes: (i) x,-1+y,z; (ii) -1+x,-1+y,z; (iii) -1+x,y,z				
TICC2				
O4-H4A···Cl3	0.81	2.29	3.095	172
O4-H4B···Cl2	0.81	2.26	3.065	176
N20-H20A···Cl2	0.86	2.49	3.299	158
N20-H20B···Cl3 [i]	0.86	2.56	3.306	145
N40-H40B···Cl2	086	2.46	3.229	149
N59-H59B···Cl3 [ii]	0.86	2.50	3.308	157
Symmetry codes: (i) -1+x,y,z; (ii) 1+x,y,z				
TICC3				
N13-H13A···Cl2 [i]	0.86	2.67	3.443	151
N13-H13B···Cl3 [ii]	0.86	2.52	3.273	146
N25-H25B···Cl2 [ii]	0.86	2.50	3.261	148
N36-H36A···Cl3 [iii]	0.86	2.56	3.285	143
N36-H36B···Cl2 [iv]	086	2.46	3.269	156
O37-H37A···Cl3 [ii]	0.78	2.23	2.991	169
O37-H37B···Cl2 [ii]	0.82	2.22	3.025	167
Symmetry codes: (i) -1+x,-1+y,z; (ii) -1+x,y,z; (iii) x,1+y,z; (iV) x,-1+y,z				

Solid-state reaction scheme and phase diagrams for all TICCs

The reaction scheme and ternary solid-state phase diagram is shown in the main text for the LEV-INA-$CaCl_2$ system. LAG results are shown here.

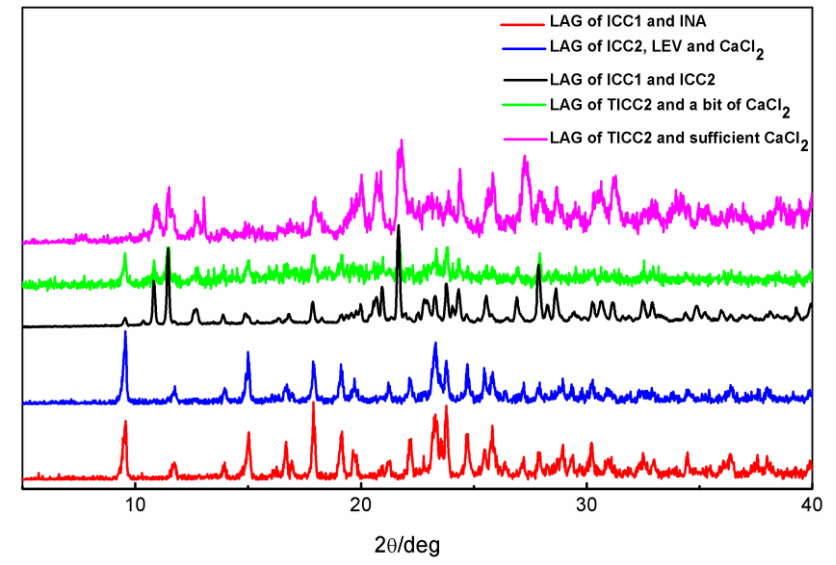

Figure S9. LAG results for the LEV-INA-$CaCl_2$ system using different starting materials and compositions.

The same experiments were applied for the ETI-INA-$CaCl_2$ and LEV-NA-$CaCl_2$ systems to investigate the solid-state thermodynamics. The XRPD experimental results, graphic scheme and the ternary phase diagrams are shown in the following.

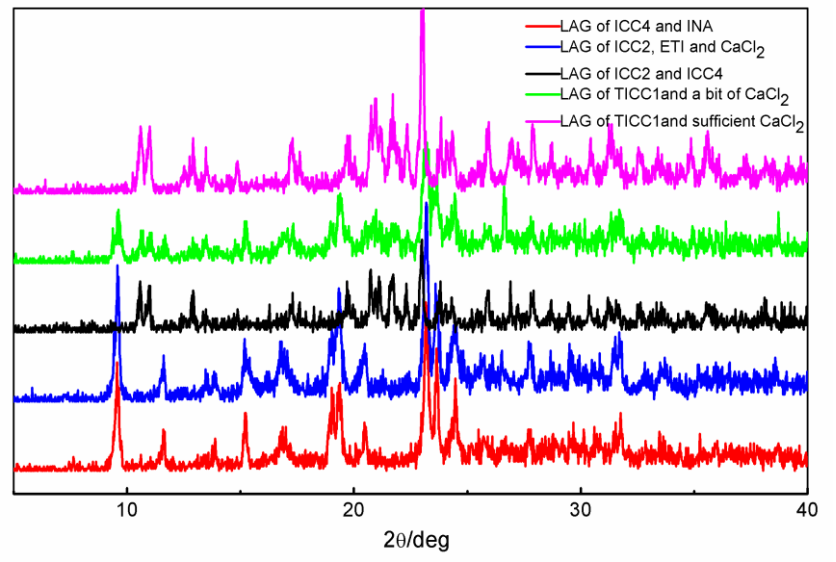

Figure S10. LAG results for the ETI-INA-$CaCl_2$ system using different starting materials and compositions.

Scheme S1. Graphic representation of reaction scheme for the ETI-INA-$CaCl_2$ system in the solid-state.

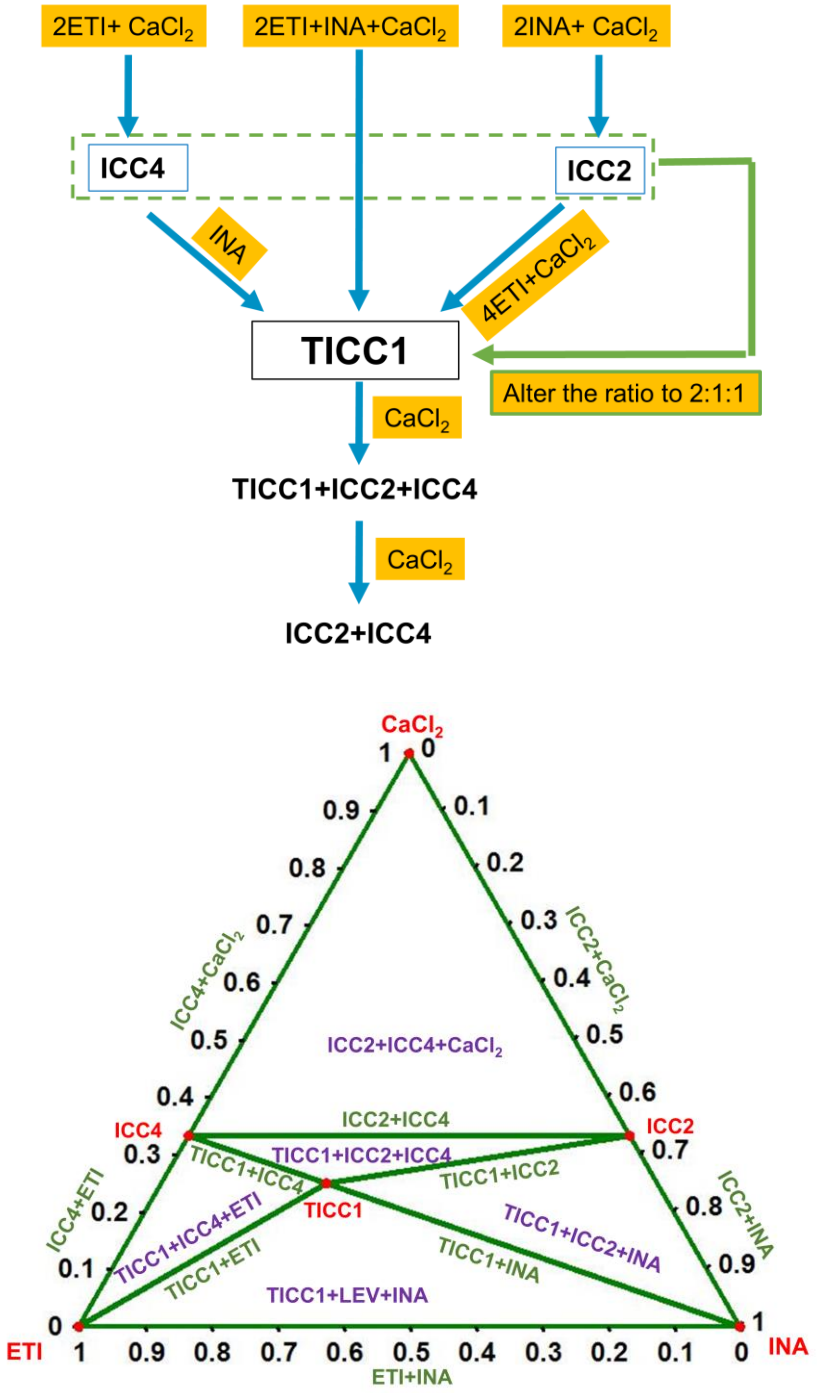

Figure S11. Ternary solid-state phase diagram for the ETI-INA-$CaCl_2$ system. Pure phases are indicated in black, mixtures of two phases in green and mixtures of three phases in purple.

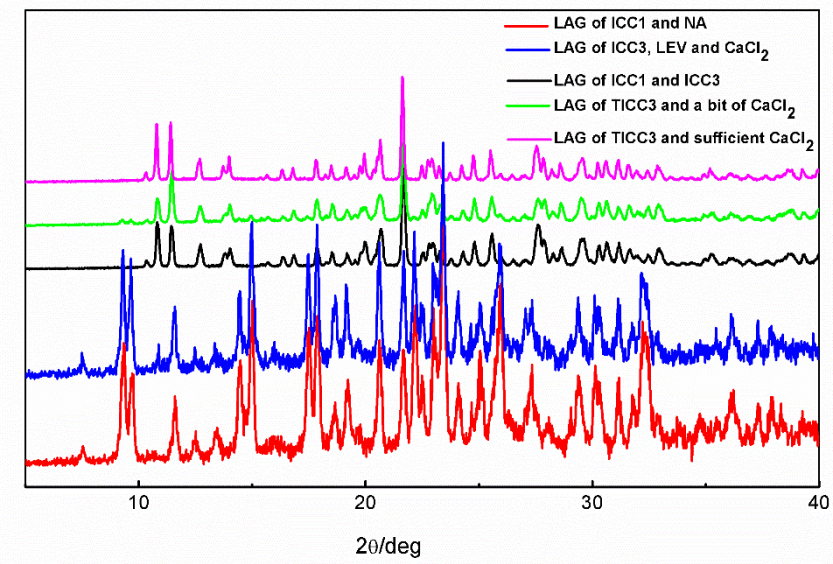

Figure S12. LAG results of the LEV-NA-$CaCl_2$ system using different starting materials and compositions.

Scheme S2. Graphic representation of the solid-state reaction scheme for the LEV-INA-CaCl2 system.

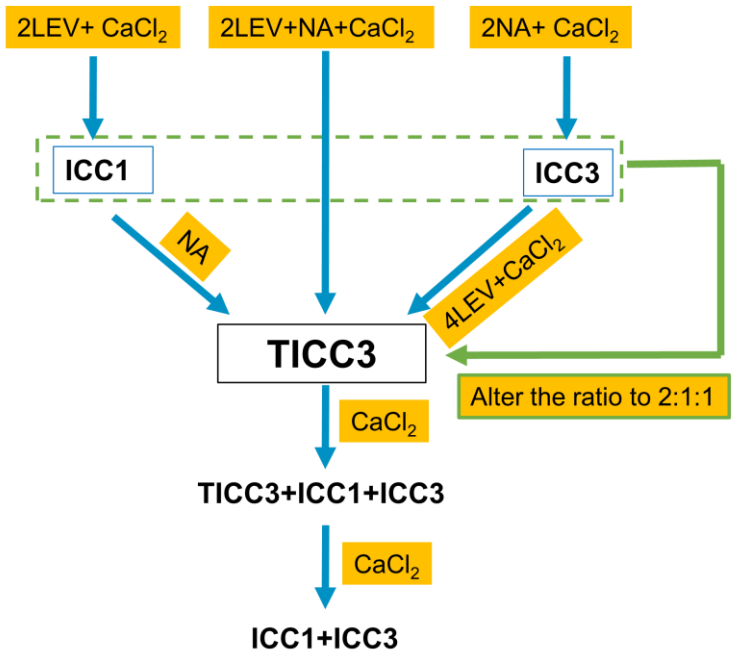

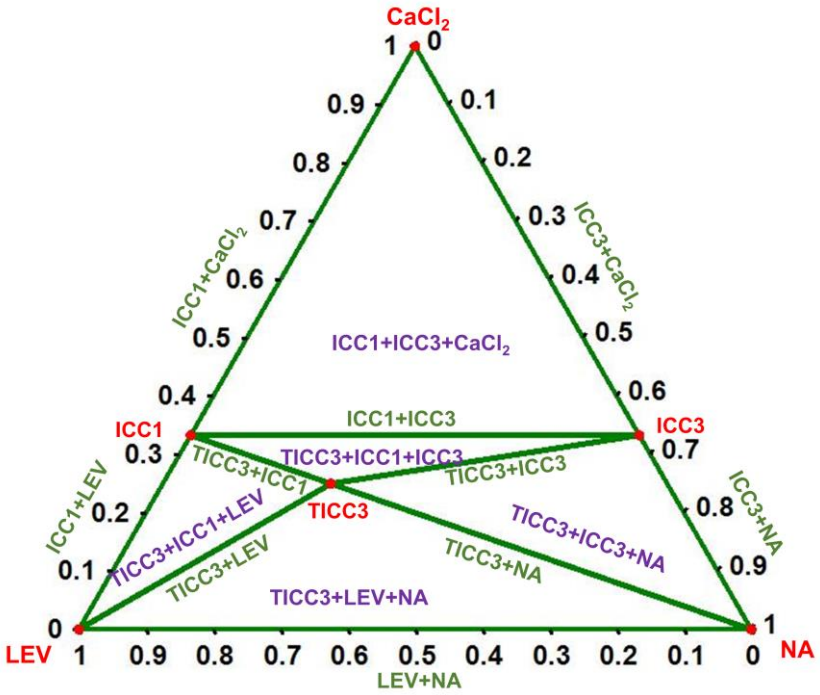

Figure S13. Ternary solid-state phase diagram for the LEV-NA-$CaCl_2$ system. Pure phases are indicated in black, mixtures of two phases in green and mixtures of three phases in purple.

Starting with a 2:1 ratio of ETI:$CaCl_2$ or NA:$CaCl_2$, the binary ionic cocrystals ICC4 or ICC3 are obtained respectively. No matter the stoichiometry of starting materials, a TICC cannot be formed. Grinding the mixture of ETI, $CaCl_2$ and ICC3 leads to the mixture of ICC4 and NA, which means ICC4 is more stable than ICC3 (Scheme S3).

Scheme S3. Graphic representation of the solid-state reaction scheme for the ETI-NA-$CaCl_2$ system.

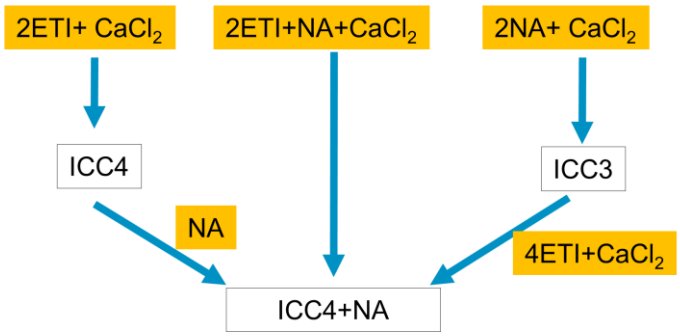

Thermal behavior of the TICCs

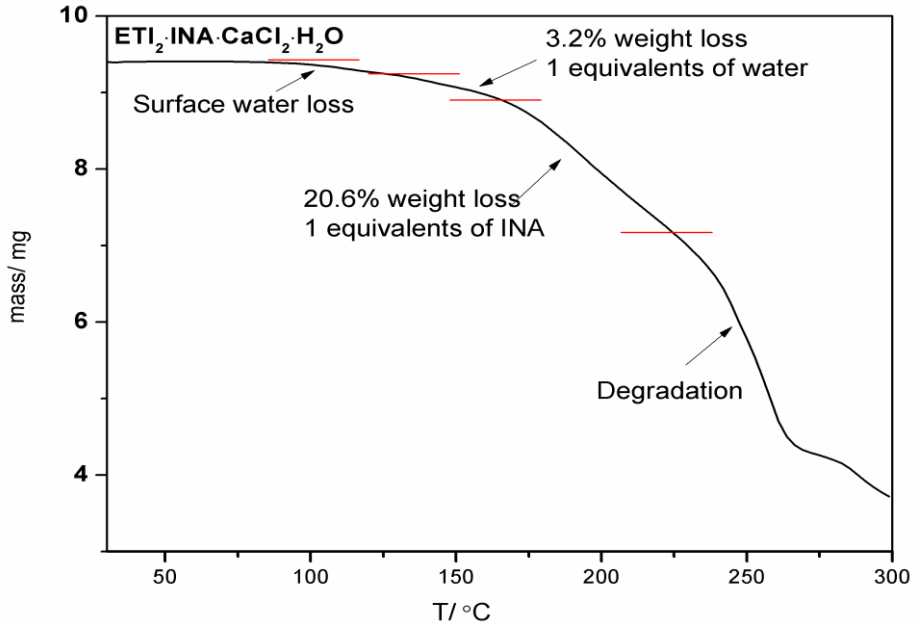

Figure S14. TGA of TICC1.

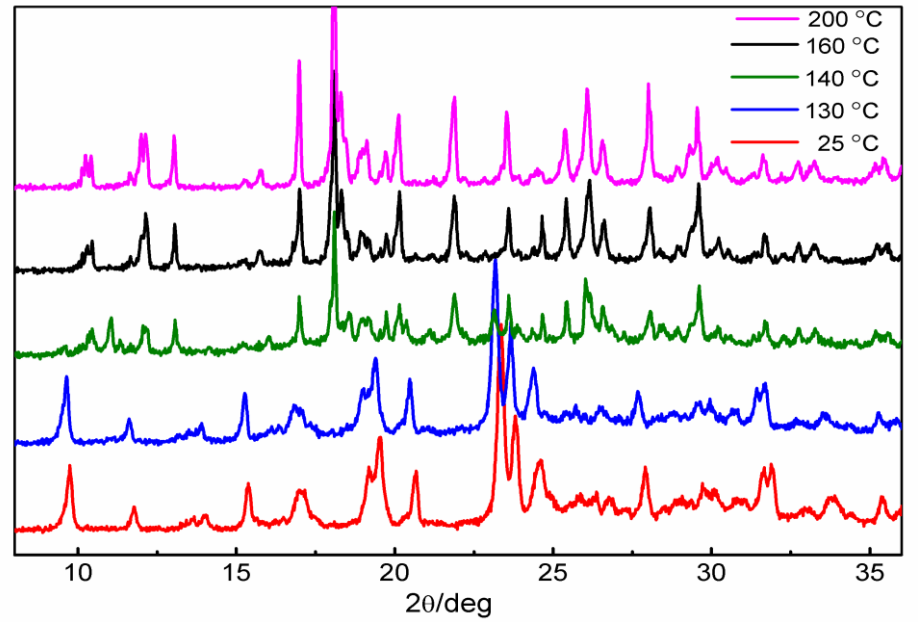

Figure S15. VT-XRPD of TICC1.

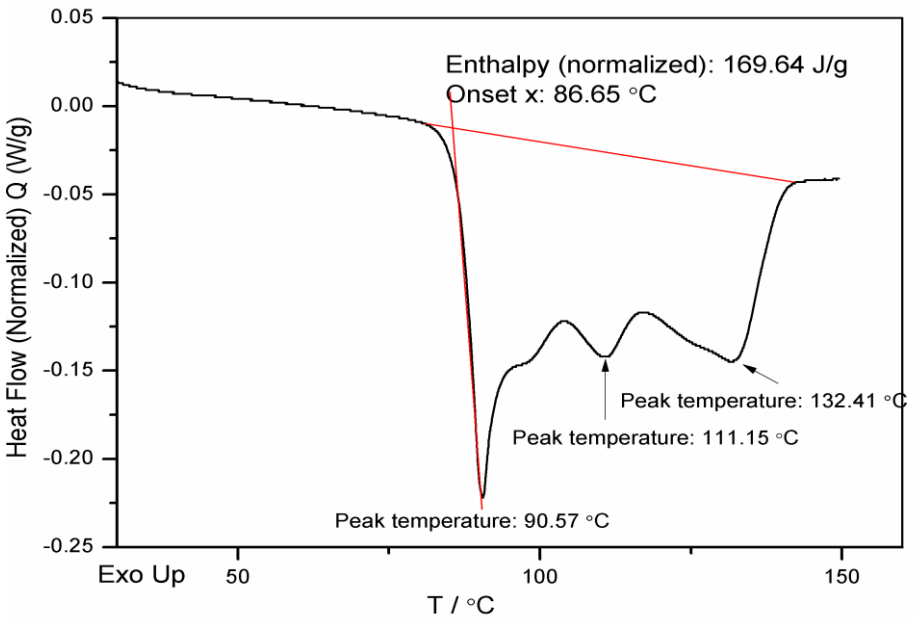

Figure S16. DSC of TICC1.

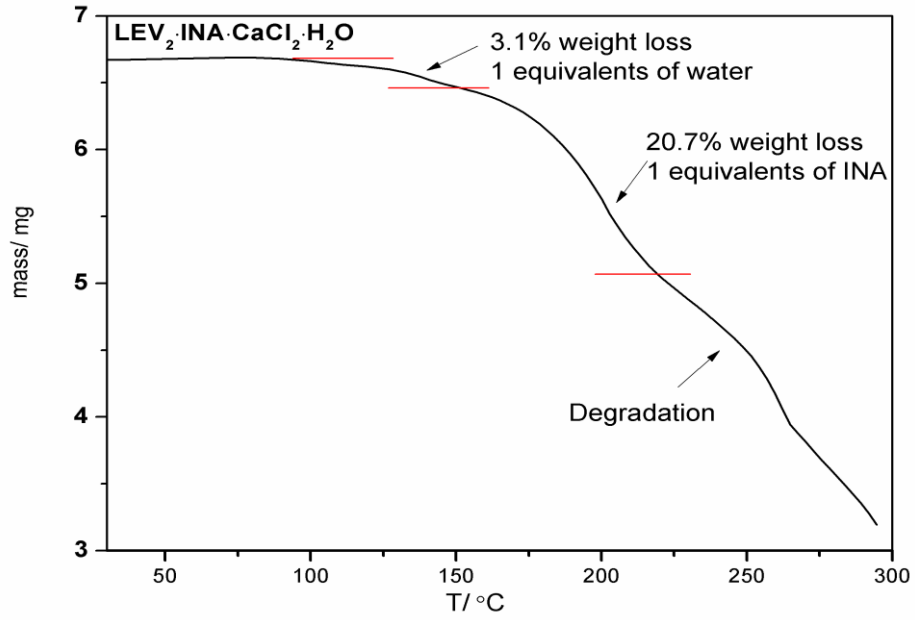

Figure S17. TGA of TICC2.

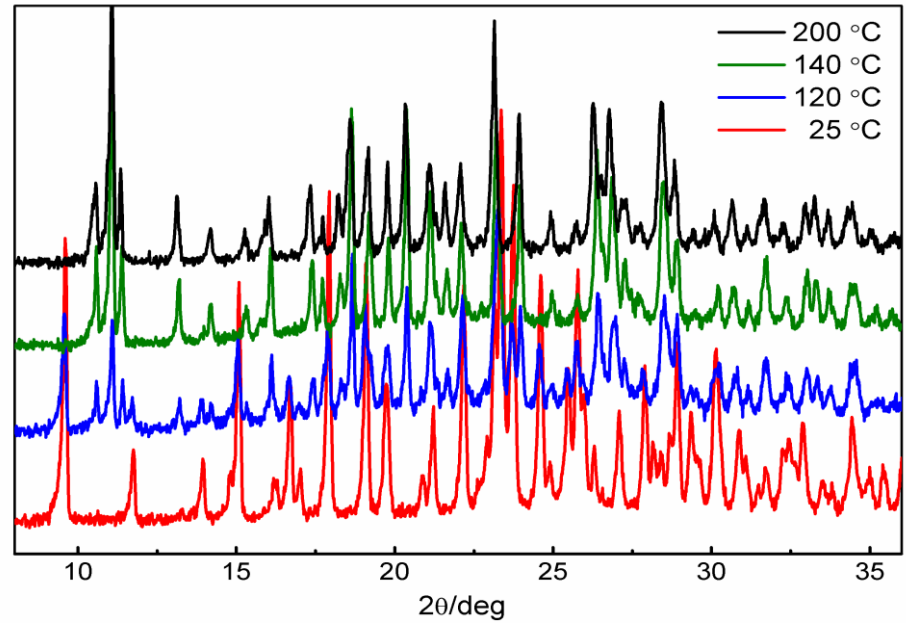

Figure S18. VT-XRPD of TICC2.

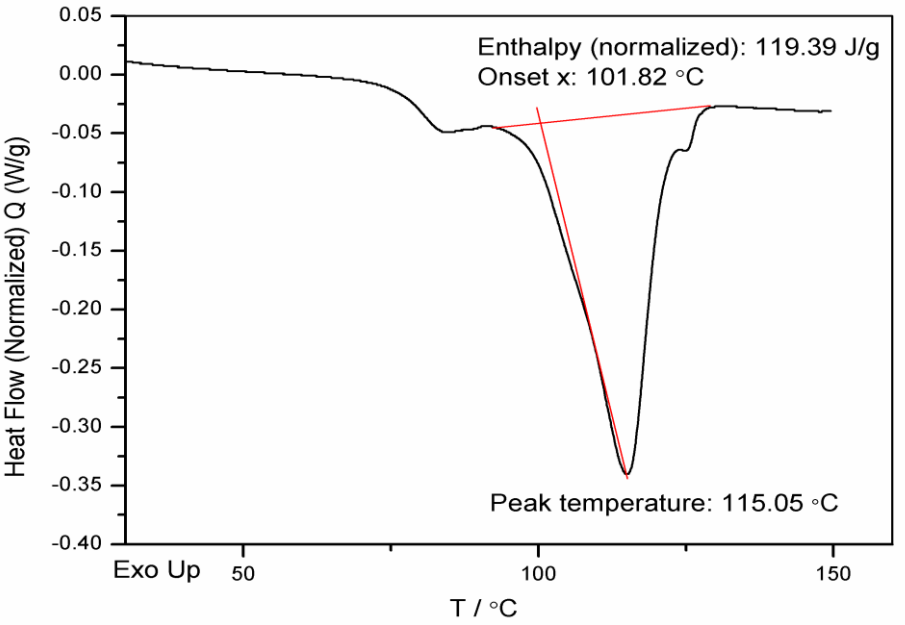

Figure S19. DSC of TICC2.

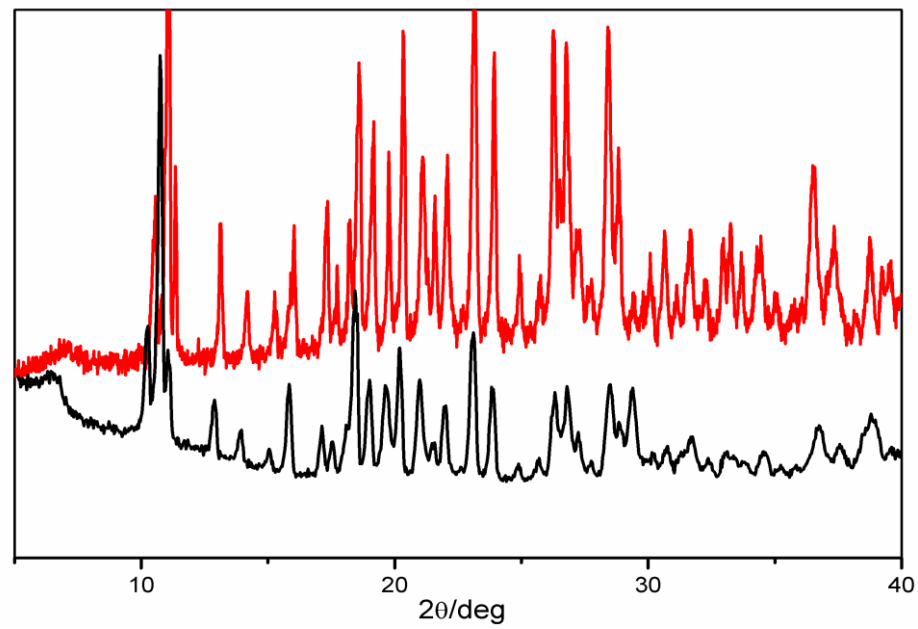

Figure S20. XRPD of TICC2 (red) and ICC1 (black) at 200 °C (different devices were used for both).

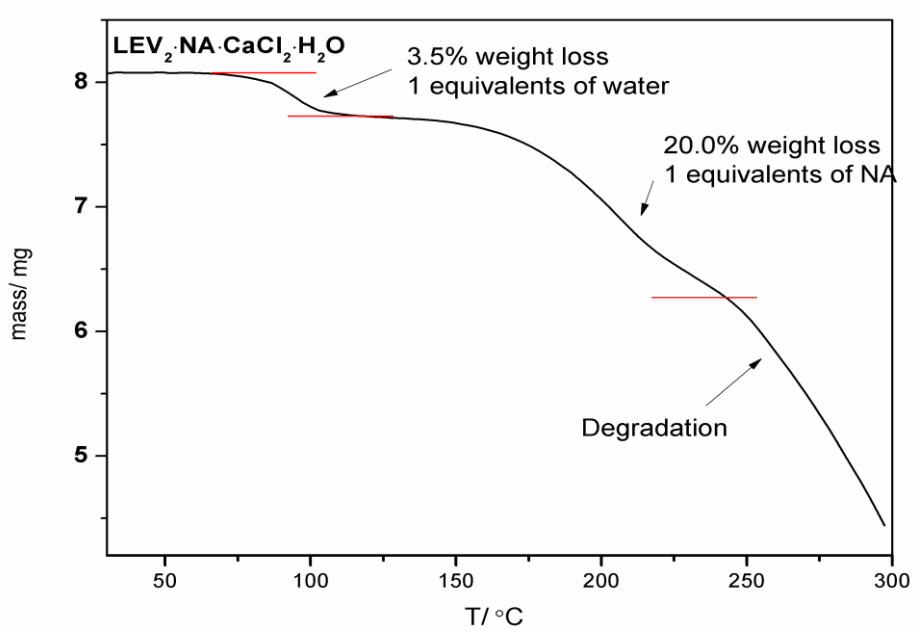

Figure S21. TGA of TICC3.

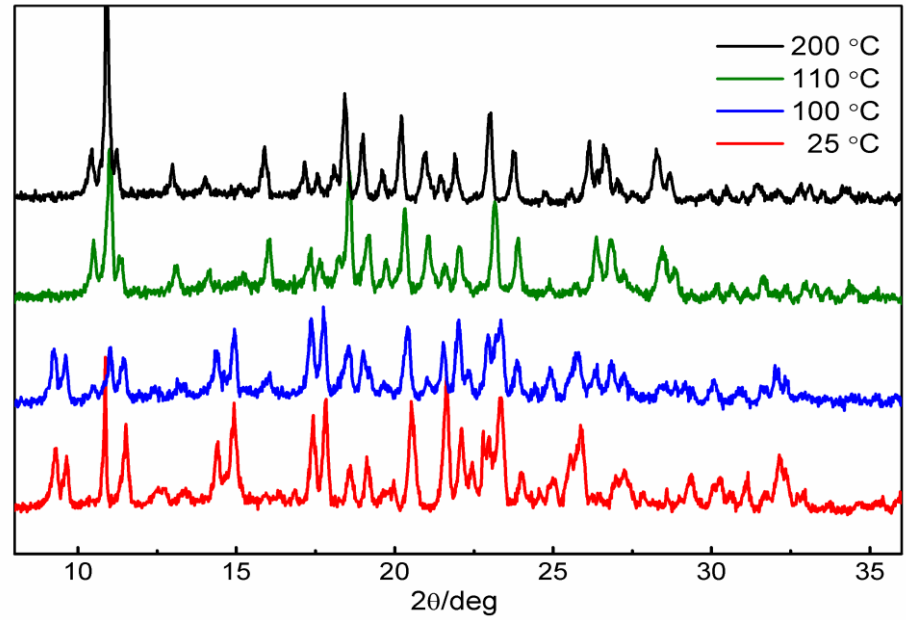

Figure S22. VT-XRPD of TICC3.

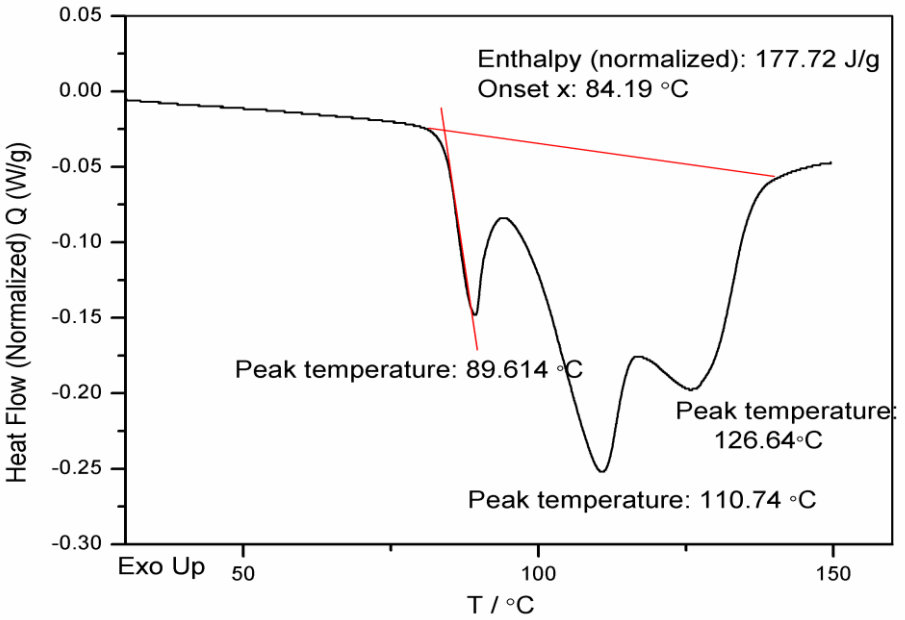

Figure S23. DSC of TICC3.

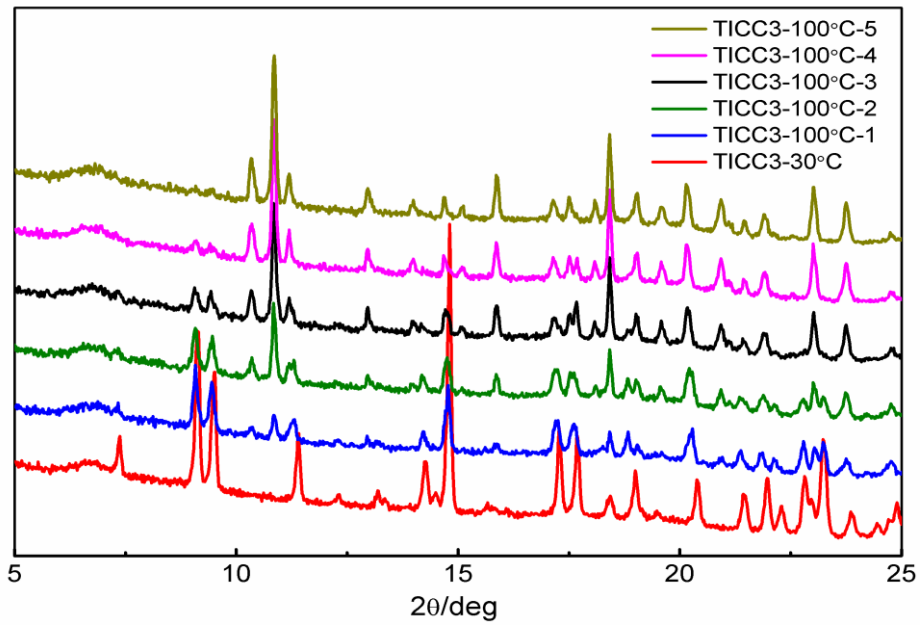

Figure S24. Isothermal hold of TICC3 at 100°C, illustrating the decomposition of the TICC in a binary anhydrous ICC and NA at 100 °C.

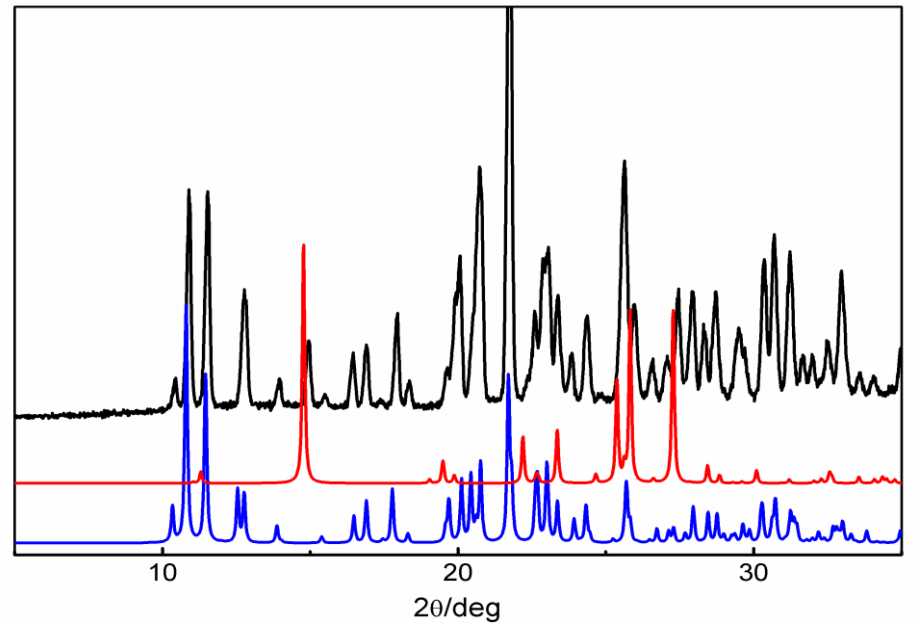

Figure S25. XRPD result of the powder recovered after having kept TICC3 for a prolonged period at 100 °C (see Figure S24). Recovered TICC3 under ambient conditions (black), simulated ICC1 (blue) and NA (red).

Solution behavior of TICCs

Table S4. Slurry results in different solvents for binary and ternary systems

Solvent	LEV+$CaCl_2$ (2:1)	INA+ $CaCl_2$ (2:1)	NA+ $CaCl_2$ (2:1)	ETI+$CaCl_2$ (2:1)	ETI+INA+$CaCl_2$ (2:1:1)	LEV+INA+$CaCl_2$ (2:1:1)	LEV+NA+$CaCl_2$ (2:1:1)
Water	ICC1+LEV	INA	ICC3	ICC4+ETI	ICC4	TICC2	ICC1+NA
Methanol	ICC1+LEV	ICC2+INA	ICC3+NA	ICC4+ETI	TICC1	TICC2	TICC3+ICC1
Ethanol	ICC1+LEV	ICC2+INA	ICC3	ICC4+ETI	TICC1	TICC2	TICC3+ICC1
Acetone	ICC1+LEV	ICC2+INA	ICC3+NA	ICC4+ETI	TICC1+ ICC4	TICC2	TICC3
Isopropanol	ICC1+LEV	ICC2+INA	ICC3	ICC4+ETI	TICC1+ ICC4	TICC2+ICC1	TICC3+ICC1
Chloroform	ICC1+LEV	INA	ICC3+NA	ICC4+ETI	TICC1+ ICC4	TICC2+LEV	TICC3+NA
Dichloromethane	ICC1+LEV	INA	ICC3+NA	ICC4+ETI	TICC1+ ICC4	TICC2+LEV	TICC3+ICC1
Acetonitrile	ICC1+LEV	ICC2+INA	ICC3+NA	ICC4+ETI	TICC1+ ICC4	TICC2+ICC1	TICC3
Ethyl acetate	ICC1+LEV	ICC2+INA	ICC3	ICC4+ETI	ICC4	TICC2+ICC1	TICC3+ICC1
Toluene	ICC1+LEV	ICC2+INA	ICC3+NA	ICC4+ETI	ICC4	ICC1+LEV	ICC1+LEV+NA
Hexane	ICC1+LEV	INA	ICC3+NA	ICC4+ETI	ICC4	ICC1+LEV	ICC1+LEV+NA
pH 1.2 HCl	ICC1	INA	ICC3	ICC4+ETI	ICC4	TICC2	ICC1

$CaCl_2$ could crystallize out especially in some non-polar solvents, but we could not identify it by XRPD as its diffraction is always overlapping with organic compounds; We also encountered some polymorphic transitions in some cases for INA and ETI.

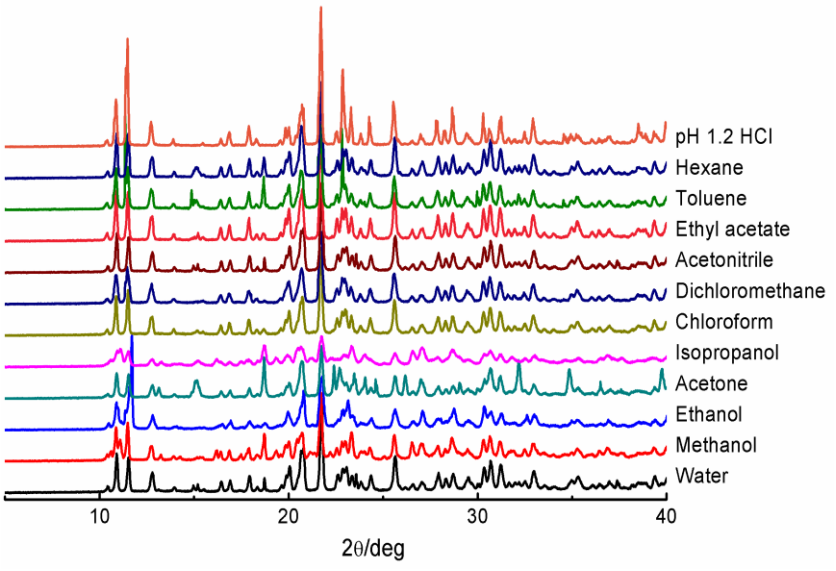

Figure S26. XRPD results of slurry experiments for the LEV-$CaCl_2$ system.

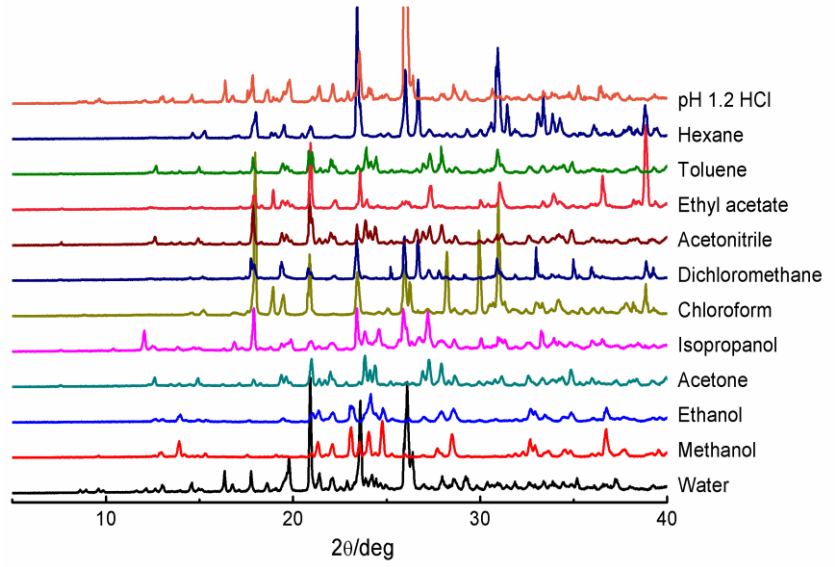

Figure S27. XRPD results of slurry experiments for the INA-$CaCl_2$ system.

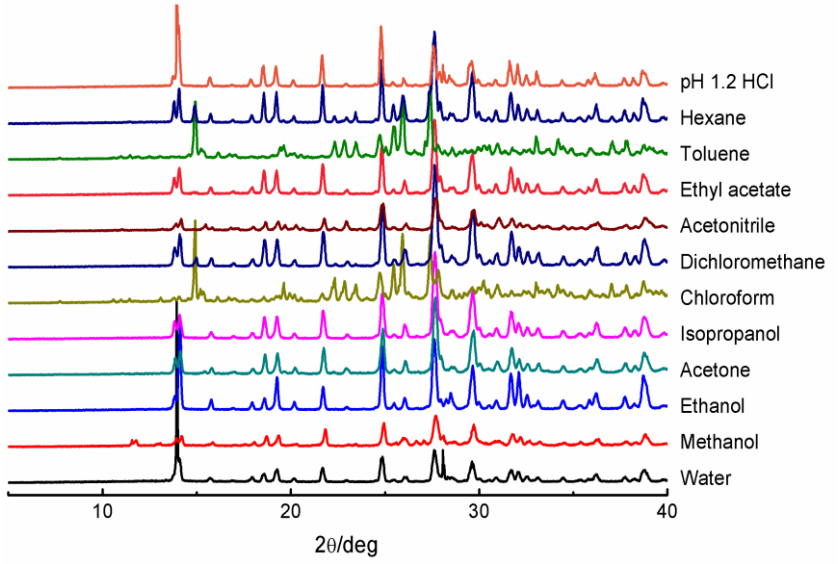

Figure S28. XRPD results of slurry experiments for the NA-$CaCl_2$ system.

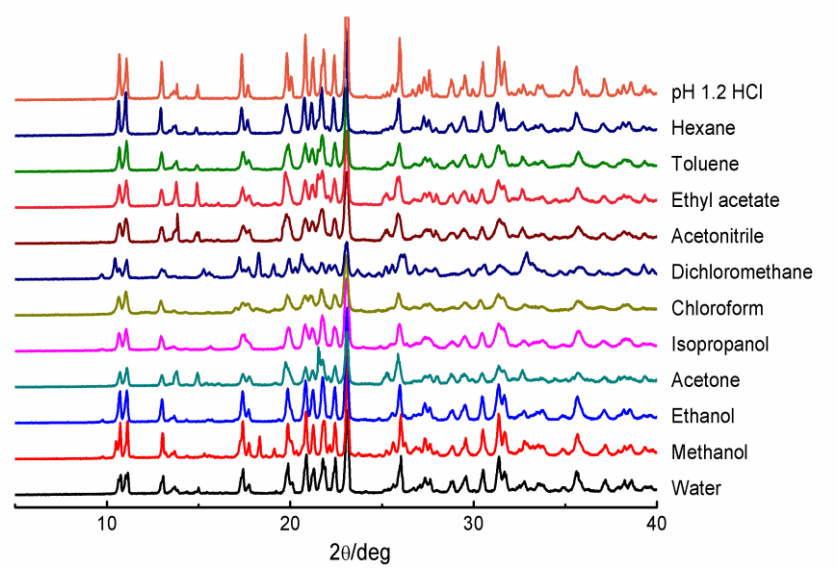

Figure S29. XRPD results of slurry experiments for the ETI-$CaCl_2$ system.

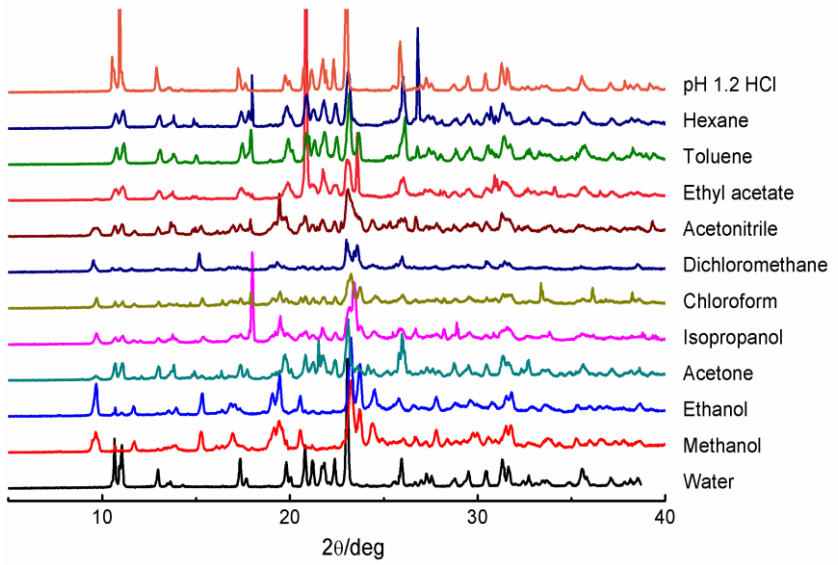

Figure S30. XRPD results of slurry experiments for the ETI-INA-$CaCl_2$ system.

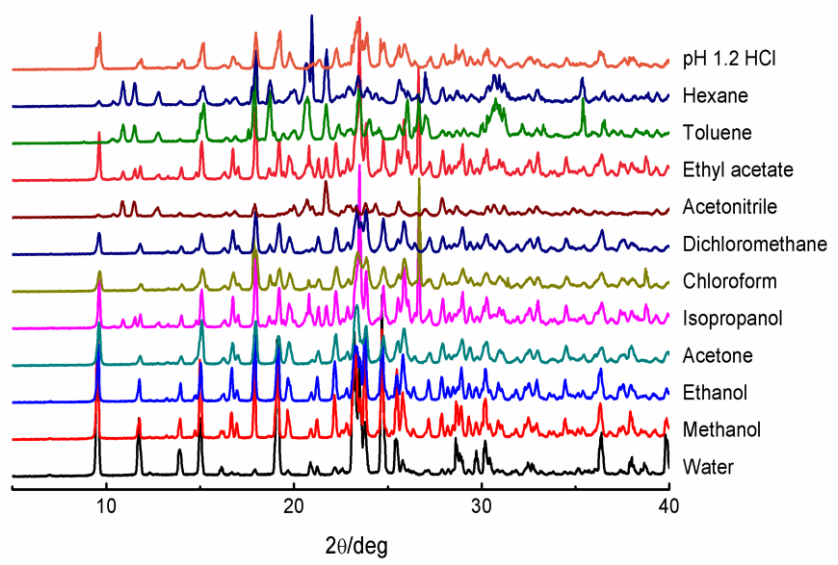

Figure S31. XRPD results of slurry experiments for the LEV-INA-$CaCl_2$ system.

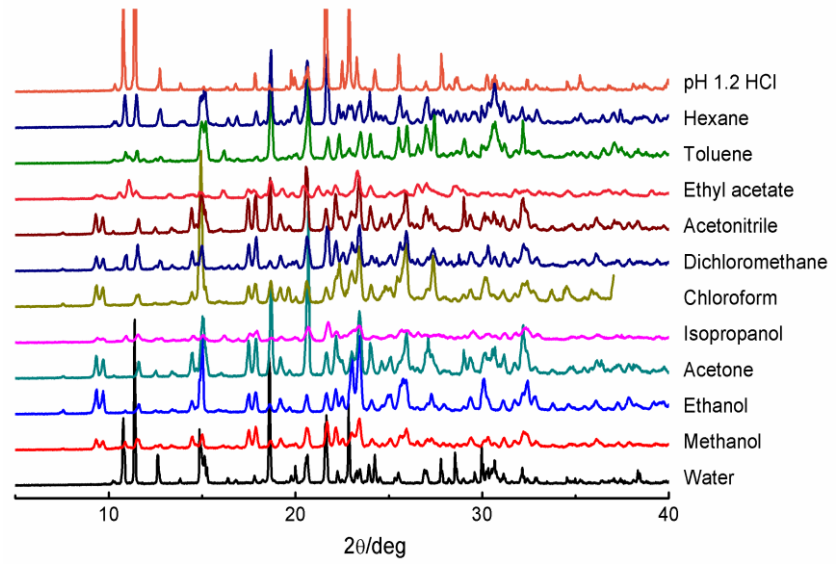

Figure S32. XRPD results of slurry experiments for the LEV-NA-$CaCl_2$ system.

Table S5. The solubility of parent compounds in different systems for different solvents at 25 °C (wt%)

Solvent	ETI	LEV	INA	NA	ICC1	ICC3	TICC1		TICC2		TICC3	
					LEV	NA	ETI	INA	LEV	INA	LEV	NA
water		51.22	10.04	43.96		45.77			40.55	14.54		
methanol	35.05	41.87	19.27				26.59	9.54	29.72	10.66		
ethanol	15.53	20.21	8.59	11.10		10.96	6.48	2.32	6.60	2.37		
acetone		5.77	3.68	4.52		2.79			7.41	2.66	5.92	2.12
acetonitrile		7.87		2.33							7.33	2.63
pH 1.2 HCl		53.69	12.72	44.20	42.71	49.95			37.21	13.35		

The blanks are the incongruent systems for which we did not perform measurements.

Experimental XRPD of binary ionic cocrystals vs calculated one from single crystal

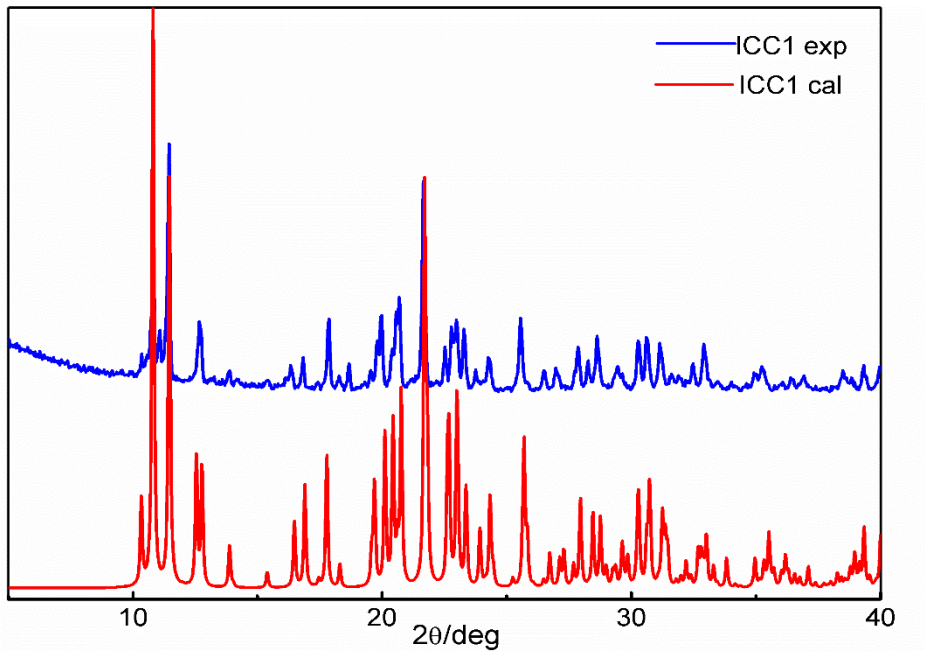

Figure S33. XRPD for ICC1. The blue one is the grinding result and the red one is the simulated one from single crystal (CCDC1894095)

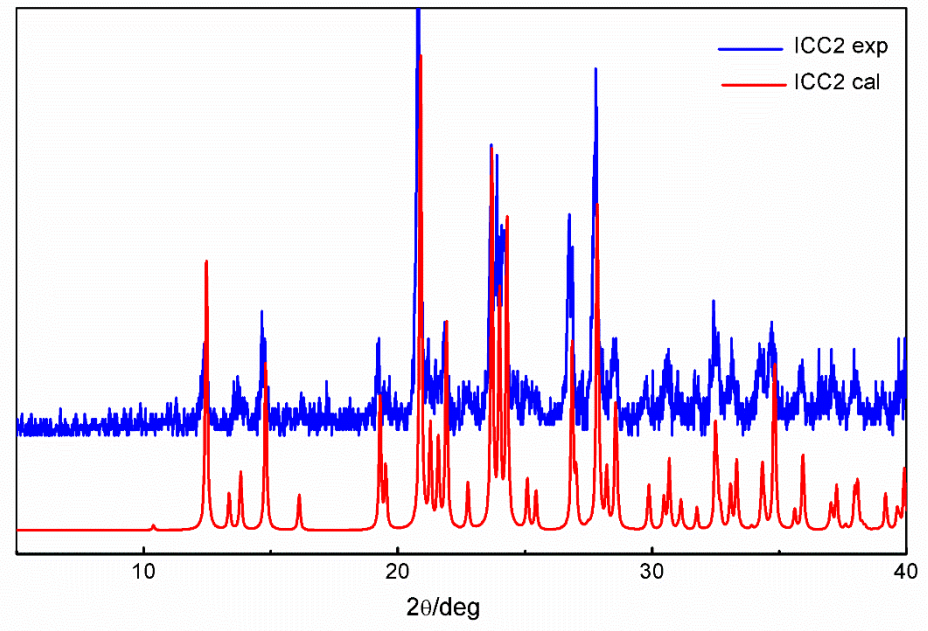

Figure S34. XRPD for ICC2. The blue one is the grinding result and the red one is the simulated one from single crystal (CCDC 1280990).

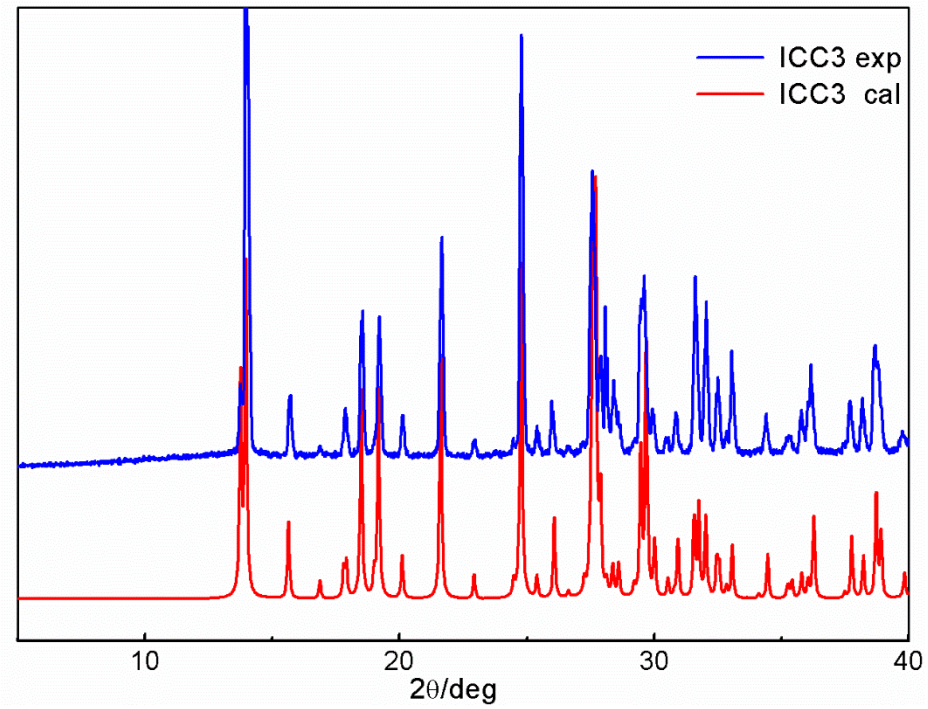

Figure S35. XRPD for ICC3. The blue one is the grinding result and the red one is the simulated one from single crystal (CCDC 949647).

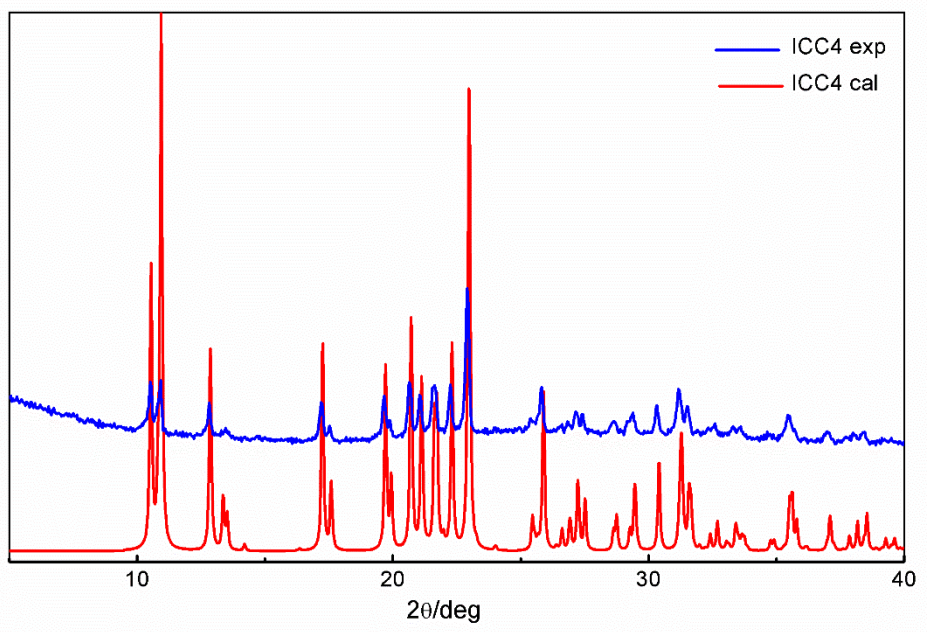

Figure S36. XRPD for ICC4. The blue one is the grinding result and the red one is the simulated one from single crystal (CCDC1894096)

References

1. C. Herman, V. Vermylen, B. Norberg, J. Wouters and T. Leyssens, Acta Crystallogr B Struct Sci Cryst Eng Mater, 2013, 69, 371-378.

2. chrysalis: Rigaku OD (2018). *CrysAlis PRO* Software system. Rigaku Corporation, Oxford, UK.

3. SHELXT: Sheldrick, G. M. (2015). *Acta Cryst.* A**71**, 3-8.

4. SHELXL: Sheldrick, G. M. (2015). *Acta Cryst.* C**71**, 3-8.

5. PLATON: Spek, A. L. (2009). *Acta Cryst.* D**65**, 148-155.